Development 134, 3615-3625 (2007) doi:10.1242/dev.006627

Fgf3 is required for dorsal patterning and morphogenesis of the inner ear epithelium

Ekaterina P. Hatch, C. Albert Noyes, Xiaofen Wang, Tracy J. Wright and Suzanne L. Mansour*

The inner ear, which contains sensory organs specialized for hearing and balance, develops from an ectodermal placode that invaginates lateral to hindbrain rhombomeres (r) 5-6 to form the otic vesicle. Under the influence of signals from intra- and extra-otic sources, the vesicle is molecularly patterned and undergoes morphogenesis and cell-type differentiation to acquire its distinct functional compartments. We show in mouse that *Fgf3*, which is expressed in the hindbrain from otic induction through endolymphatic duct outgrowth, and in the prospective neurosensory domain of the otic epithelium as morphogenesis initiates, is required for both auditory and vestibular function. We provide new morphologic data on otic dysmorphogenesis in *Fgf3* mutants, which show a range of malformations similar to those of *Mafb* (*Kreisler*), *Hoxa1* and *Gbx2* mutants, the most common phenotype being failure of endolymphatic duct and common crus formation, accompanied by epithelial dilatation and reduced cochlear coiling. The malformations have close parallels with those seen in hearing-impaired patients. The morphologic data, together with an analysis of changes in the molecular patterning of *Fgf3* mutant otic vesicles, and comparisons with other mutations affecting otic morphogenesis, allow placement of *Fgf3* between hindbrain-expressed *Hoxa1* and *Mafb*, and otic vesicle-expressed *Gbx2*, in the genetic cascade initiated by WNT signaling that leads to dorsal otic patterning and endolymphatic duct formation. Finally, we show that *Fgf3* prevents ventral expansion of r5-6 neurectodermal *Wnt3a*, serving to focus inductive WNT signals on the dorsal otic vesicle and highlighting a new example of cross-talk between the two signaling systems.

KEY WORDS: Fibroblast growth factor, Mouse mutant, Endolymphatic duct and sac, WNT signaling, Hearing and balance

INTRODUCTION

The inner ear is a morphologically complex sensory organ responsible for hearing and balance. In higher vertebrates, the sound-sensing cells are housed in the ventrally located cochlear duct and the head motion-sensing cells are housed within the dorsally located vestibular system. The vestibular system is further divided into the more dorsally located semicircular canal system, in which sensory patches devoted to angular motion detection (cristae) are found at the base (ampulla) of each of three non-sensory canal ducts, and sensory patches devoted to linear motion detection (maculae) are contained within the centrally located saccule and utricle. The inner ear also has a dorsally projecting non-sensory appendage, the endolymphatic duct and sac (EDS), which plays an important role in maintaining the unique fluid environment essential for normal sensory function of the inner ear. Dysfunction of the inner ear is among the most common congenital disorders, affecting at least 1 in 500 births (Smith et al., 2005; Morton and Nance, 2006) and up to 39% of sensorineural deafness is associated with inner ear malformations (Mafong et al., 2002; Wu et al., 2005).

In mice, inner ear formation initiates on embryonic day (E) 8.0 as a placodal thickening of head ectoderm adjacent to hindbrain rhombomeres (r) 5-6. Subsequently, from E8.5-9.0, the placode invaginates, forming the otic cup, from which neuroblasts of the eighth ganglion (GVIII) delaminate anteroventrally and migrate medially. By E9.5, the cup closes and separates from the surface ectoderm, forming the spherical otic vesicle, or otocyst. During the next 6 days, this simple, fluid-filled epithelium acquires its mature and complex morphology and begins to differentiate its multitude of distinct sensory and non-sensory cell types. Morphogenesis of the vesicle initiates at E10.5 with a dorsomedially directed outgrowth of the EDS anlage and a ventrally directed outgrowth of the cochlear duct. At E11.5, the otic epithelium evaginates dorsolaterally to form the vertical canal plate, the precursor of the anterior and posterior semicircular canals, which are separated by the common crus, and shortly thereafter evaginates laterally to form the lateral canal plate, the precursor of the lateral semicircular canal. The canals are formed at E12.5 by fusion of cells within two central regions of the vertical plate and a single central region of the lateral canal plate, followed at E13.5 by resorption of the fused cells into the epithelium. During this period, there are additional evaginations of the central region to form the more dorsally situated utricle and the more ventrally situated saccule. By E15.5, the inner ear epithelium has acquired its mature morphology, but is still undergoing cellular differentiation within the six sensory patches (Kiernan et al., 2002; Barald and Kelley, 2004; Mansour and Schoenwolf, 2005; Fritzsch et al., 2006).

The initial induction and subsequent morphogenesis and differentiation of the otic epithelium involves signaling interactions within and between otic and non-otic tissues. In particular, fibroblast growth factor (FGF) signals from the endoderm induce a mesenchymal FGF that is required together with hindbrain FGFs for expression of otic placode genes and for otic placode induction and vesicle formation. Based on genetic data, these signals are likely to be provided in mice by FGF8, FGF10 and FGF3, expressed by the endoderm, mesenchyme and hindbrain, respectively (Alvarez et al., 2003; Wright and Mansour, 2003; Ladher et al., 2005; Zelarayan et al., 2007). WNT signals, presumably from the hindbrain, are required to limit the region of the ectoderm that forms the otic placode (Ohyama et al., 2006). In response to the inductive signals, the otic placode expresses several transcription factor genes uniformly, including *Pax2*, *Dlx5* and *Gbx2* (Wright and Mansour, 2003; Ladher et al., 2005). By the otocyst stage, the expression

Department of Human Genetics, University of Utah, Salt Lake City, UT 84112-5330, USA.

*Author for correspondence (e-mail: suzi.mansour@genetics.utah.edu)

Accepted 27 July 2007

domains of most otic markers become confined to restricted domains of the vesicle specified to give rise to different ear structures (Fekete and Wu, 2002). This division of the otocyst into gene expression domains required for normal morphogenesis also depends on signals from the hindbrain. Removal or rotation of the neural tube in the vicinity of the developing otic tissue or rotation of the vesicle disrupts otic vesicle molecular patterning and development, particularly the outgrowth of the EDS and cochlear duct (Hutson et al., 1999; Bok et al., 2005). Mutations in hindbrain-expressed genes, such as *Mafb* (*Kreisler*) and *Hoxa1*, which cause defects in the development of r5-6, also show aberrant patterning of the otic vesicle that presages inner ear malformations (Pasqualetti et al., 2001; Choo et al., 2006). WNT signaling from the hindbrain is sufficient to maintain the expression of some dorsal otic genes, and *Wnt1* and *Wnt3a*, which are expressed in the dorsal hindbrain, are required redundantly for formation of the vestibular structures (Riccomagno et al., 2005).

FGF signaling is also implicated in otic vesicle morphogenesis. FGF3 and FGF10 are expressed by prospective otic sensory tissues (Wilkinson et al., 1988; Mahmood et al., 1996; McKay et al., 1996; Pirvola et al., 2000; Pauley et al., 2003), and their major receptor, FGFR2b, is found in prospective non-sensory tissue (Pirvola et al., 2000). Global inhibition of FGF signaling by application of SU5402 to chick E2.5-3 otic vesicles just prior to semicircular canal pouch evagination causes dose-dependent inhibition of canal formation, suggesting that developing sensory structures control morphogenesis of non-sensory structures (Chang et al., 2004). Mouse mutants support this concept. Mice lacking FGFR2b form otic vesicles that subsequently develop dysmorphologies initiating at EDS outgrowth and include failure of semicircular canal formation (Pirvola et al., 2000). Most *Fgf10* mutants completely lack semicircular canals (Pauley et al., 2003; Ohuchi et al., 2005). *Fgf3*-null mutants undergo normal otic vesicle formation, but then go on to develop highly variable and incompletely penetrant inner ear dysmorphologies that, like those of *Fgfr2b* mutants, appear to initiate at the EDS outgrowth stage. These mutants also show a reduction in the size of GVIII (Mansour et al., 1993).

To gain insight into the mechanism of *Fgf3* function in otic morphogenesis, we determined the three-dimensional structure of *Fgf3* mutant ears and the changes in their molecular patterning. We show that homozygous mutants have variably penetrant and expressive inner ear morphologies that are characterized most typically by loss of the EDS and common crus, dilatation of the remaining epithelium and poor coiling of the cochlea, phenotypes that are very similar to those of *Hoxa1*, *Mafb* and *Gbx2* mutants (Pasqualetti et al., 2001; Lin et al., 2005; Choo et al., 2006) as well as to some classes of hearing-impaired patients (Manfre et al., 1997; Kim et al., 2004; Wu et al., 2005). The initial molecular patterning of *Fgf3* mutant otocysts was normal, but by E10-10.5 these ears lacked or had reduced domains of dorsal otic genes, suggesting a loss of the cells fated to form the EDS. Ventrally expressed genes important for cochlear development were not affected, but markers of the developing vestibular sensory domains, particularly those expressed in the posterior otic vesicle, were downregulated or absent and GVIII was reduced and displaced dorsomedially. Finally, hindbrain expression of *Wnt3a* was ventrally expanded in *Fgf3* mutants. Taken together, our results show that *Fgf3* is required for dorsal otic patterning and that its primary role is to sustain and focus the dorsal otic gene expression induced by WNT signals. We suggest that *Fgf3* also serves to focus inductive WNT signals on the dorsal otic vesicle, highlighting a new example of cross-talk between the two signaling systems.

MATERIALS AND METHODS

Fgf3 alleles and genotyping

All mouse use complied with protocols approved by the University of Utah Institutional Animal Care and Use Committee. The targeted $Fgf3^{neo}$ allele ($Fgf3^{tm1Mrc}$, MGI:1931059) was described previously and has an insertion of a promoter-containing *Neo* gene in the first protein-coding exon (1B) (Mansour et al., 1993). A new *Fgf3* allele ($Fgf3^{\Delta 2}$), which has a deletion of exon 2, was generated by first targeting loxP sites on either side of exon 2 to generate a conditional allele and then deleting the intervening DNA using CRE recombinase (X.W. and S.L.M., unpublished). $Fgf3^{\Delta 2}$ transcripts contain exon 1 spliced directly to exon 3, which is in a different frame. Thus, they encode only the first 73 of 245 FGF3 amino acids, including only the first 28 of 137 amino acids of the FGF core homology domain.

Both *Fgf3* alleles were studied on a mixed genetic background containing hybrid 129 and C57Bl/6 alleles. Genotypes of heterozygous intercross offspring were determined by PCR amplification of yolk sac or tail DNA using three-primer mixes that distinguish the mutant and wild-type alleles. The $Fgf3^{neo}$ genotyping assay was performed as described previously (Wright and Mansour, 2003). The $Fgf3^{\Delta 2}$ genotyping mix, containing primers 455C (5′-CTGCCTATGTGCTATATCCATGG-3′), 456C (5′-GTAGATGACTGAGTGTGTAGG-3′) and 485B (5′-GGTTCCTCGA-TCAAACTCTGG-3′), was amplified in an MJR thermocycler for 35 cycles of 30 seconds at 94°C, 20 seconds at 60°C and 1 minute at 72°C and produced a wild-type band of 250 bp and a mutant band of 600 bp.

Paint-filling and RNA in situ hybridization

E15.5 paint-filled ears were prepared as described (Morsli et al., 1998). Otic and hindbrain marker gene expression was detected in somite-stage matched E9.5-10.5 (the day of vaginal plug detection was regarded as E0.5) specimens by whole-mount in situ hybridization with digoxigenin-labeled antisense cRNA probes as described (Henrique et al., 1995). Hybridization probes were generated from plasmids containing: *Pax2* (Dressler et al., 1990), *Dlx5* (Depew et al., 1999), *Gbx2* (Wassarman et al., 1997), *Hmx3* (*Nkx5.1*) (Merlo et al., 2002), *Lfng* (Morsli et al., 1998), *Fgf10* (Xu et al., 1998), *Wnt1* and *Wnt3a* (Parr et al., 1993), *Wnt2b* (Grove et al., 1998), *Bmp4* (Jones et al., 1991), *Otx2* (Simeone et al., 1993) *Mafb* (Cordes and Barsh, 1994) and *Gata3* (George et al., 1994). Stained embryos were cryoprotected in sucrose and cryosectioned as described (Stark et al., 2000). Two to six embryos of each genotype were analyzed with each probe.

Auditory brainstem response threshold measurements

Mice were anesthetized using 0.02 ml/g avertin. Auditory brainstem response (ABR) thresholds for click stimuli (47 μsecond duration, 29.3/second) presented to each ear individually, were determined using high-frequency transducers controlled and analyzed by SmartEP software (Intelligent Hearing Systems) according to Zheng et al. (Zheng et al., 1999).

RESULTS

We showed previously that $Fgf3^{neo/neo}$ mice have defects of inner ear morphogenesis that are incompletely penetrant and variably expressive. The earliest morphologic defect was a failure of EDS outgrowth between E9.5 and E10.5 (Mansour et al., 1993). Here we present a more detailed analysis of the inner ear dysmorphology in *Fgf3* mutants and an analysis of otic marker genes using the previously described $Fgf3^{neo}$ allele and a newly targeted $Fgf3^{\Delta 2}$ allele (Fig. 1A).

$Fgf3^{neo}$ and $Fgf3^{\Delta 2}$ adult homozygotes have similar survival and gross skeletal and otic phenotypes

To determine whether the new $Fgf3^{\Delta 2}$ allele was similar to the $Fgf3^{neo}$ allele, we first compared the phenotypes of adult homozygotes. Offspring of $Fgf3^{+/neo}$ and $Fgf3^{+/\Delta 2}$ intercrosses were observed and genotyped at weaning. In both cases, although all three genotypes were recovered, the genotypic distribution deviated significantly from the normal mendelian expectation (Fig. 1B). Only

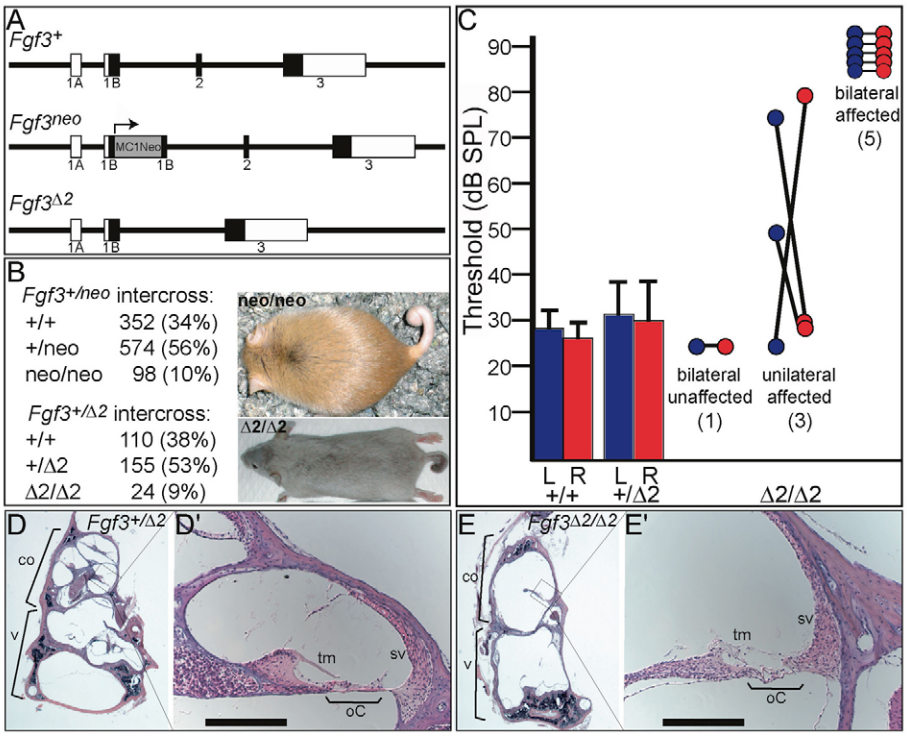

Fig. 1. *Fgf3* alleles and adult phenotypes. (**A**) Depiction of wild-type (*Fgf3*$^{+}$), original (*Fgf3*^{neo}) and newly targeted (*Fgf3*$^{\Delta 2}$) *Fgf3* alleles. Solid lines, mouse genomic *Fgf3* DNA; open boxes, untranslated regions; solid boxes, protein-coding regions; gray box, MC1Neo cassette. (**B**) Genotypes at weaning of *Fgf3*$^{+/neo}$ and *Fgf3*$^{+/\Delta 2}$ intercrosses. Numbers and percentage of total (in parentheses) for wild-type (+/+), heterozygous (+/neo or +/Δ2) and homozygous (neo/neo or Δ2/Δ2; photographs to the right) offspring are shown. (**C**) Auditory brainstem response (ABR) thresholds of *Fgf3*$^{+/\Delta 2}$ intercross offspring. Average thresholds (in decibels sound pressure level) for left (L, blue) and right (R, red) ears of +/+ (n=7) and +/Δ2 (n=12) animals are shown as boxes; bars indicate one standard deviation. Homozygous mutant (Δ2/Δ2) ABR measurements are presented as connected circles (left, blue; right, red) for individual animals, with numbers in parentheses indicating the total number of mutant animals with the specified phenotype. Low (**D**,**E**) and high (**D′**,**E′**) magnification views of Hematoxylin and Eosin-stained mid-modiolar sections of *Fgf3*$^{+/\Delta 2}$ (hearing, D,D′) and *Fgf3*$^{\Delta 2/\Delta 2}$ (deaf, E,E′) ears. oC, organ of Corti; sv, stria vascularis; tm, tectorial membrane. Scale bars: 50 μm.

10% of *Fgf3*$^{+/neo}$ and 9% of *Fgf3*$^{+/\Delta 2}$ intercross offspring were homozygous mutant, showing that there is significant and similar lethality associated with both alleles. In addition, all homozygous mutants exhibited the characteristic short, curly tails described previously (Fig. 1B) (Mansour et al., 1993). Thus, the two *Fgf3* alleles behave similarly at the overt phenotypic level.

Some of the previously described *Fgf3*$^{neo/neo}$ animals had an abnormal Preyer's reflex and exhibited circling behavior, which suggested auditory and vestibular dysfunction (Mansour et al., 1993). Therefore, we measured auditory brainstem response (ABR) thresholds in each ear in 6-week-old animals of all three *Fgf3*$^{\Delta 2}$ genotypes. No significant differences in auditory thresholds were observed between wild-type (n=7) and heterozygous (n=11) animals and all of these controls had normal behavior. By contrast, only one *Fgf3*$^{\Delta 2/\Delta 2}$ animal had normal thresholds in both ears and eight of nine *Fgf3*$^{\Delta 2/\Delta 2}$ animals had ABR thresholds that were significantly elevated (>2 standard deviations above same-side controls) in one (n=3) or both (n=5) ears (Fig. 1C). All five bilaterally affected homozygous mutants showed circling behavior, whereas the three unilaterally affected animals had only a slight head tilt. Histological sections of normal-hearing heterozygous inner ears showed typical gross morphology and normal cochlear structure (Fig. 1D,D′). By contrast, inner ear sections of a deaf homozygote showed only rudimentary partitioning into distended cochlear and vestibular chambers. Nevertheless, the otic epithelium could be identified and showed evidence of sensory differentiation, albeit abnormal (Fig. 1E,E′). Thus, as was concluded using morphologic studies of *Fgf3*^{neo} homozygotes (Mansour et al., 1993), *Fgf3*$^{\Delta 2}$ homozygotes have auditory and vestibular phenotypes that are incompletely penetrant and variably expressive.

Most *Fgf3* mutants show abnormal otic morphologies

To visualize more clearly the consequences of loss of *Fgf3* to inner ear morphogenesis, we filled E15.5 *Fgf3* control (Fig. 2A,B) and mutant (Fig. 2C-I) inner ear epithelia with latex paint. Both *Fgf3* alleles were studied, but no obvious differences between them were apparent, so the results for a total of 120 mutant ears were combined. At the gross anatomical level, 50/120 (42%) of mutant ears had a normal morphology, consistent with incomplete penetrance of the adult *Fgf3* auditory and vestibular phenotypes (Fig. 2C). The remaining 70 (58%) showed graded morphologic defects that were assigned to groups based on the classification of *Gbx2*-null ears (Lin et al., 2005).

Virtually all affected *Fgf3* mutant ears had a distended membranous labyrinth (n=65/70). In most cases, the swollen cochlear duct showed incomplete partition and poor coiling. All of the expected structures could be identified in type Ia ears, but the endolymphatic duct appeared truncated dorsally, lacking the endolymphatic sac (Fig. 2D, n=8/70). Type Ib ears were similar to type Ia, but entirely lacked the EDS appendage (Fig. 2E, n=12/70). Type II was the most common phenotype seen in affected *Fgf3*

mutant ears and included absence of the EDS as well as of the common crus, such that the anterior and posterior canals appeared as a single continuous canal (Fig. 2F, *n*=32/70). In addition, the utricle and saccule were fused with the enlarged cochlear duct. Smaller numbers of mutant ears were even more severely affected. Type III ears had the EDS and common crus aplasia typical of type II ears, together with absence or severe truncation of the anterior and posterior semicircular canals (Fig. 2G, *n*=5/70). Most of the associated ampullae could be identified, but one ear lacked the posterior ampulla and another lacked the anterior ampulla. These ears all retained the lateral canal and ampulla. The type III cochlear duct was severely malformed and shortened, with less than one coil. The type IV phenotype was the most severe, with defects in all inner ear structures. The only discernible formation was a cochlea-like structure (Fig. 2H, *n*=7/70). Taken together, these data show that the abnormal morphologies of most *Fgf3* mutant ears included hypoplasia or aplasia of the EDS, swelling of the remaining labyrinth and, in many cases, aplasia of the common crus. These are similar to the phenotypes seen in *Hoxa1*, *Mafb* and *Gbx2* mutant ears (Pasqualetti et al., 2001; Lin et al., 2005; Choo et al., 2006).

A few affected *Fgf3* mutant ears retained a normal endolymphatic appendage and were not distended. These were grouped into type O (*n*=5/70). Three type O ears lacked the posterior canal and ampulla (Fig. 2I). One type O ear lacked the lateral canal and one had an abnormally thickened and posteriorly positioned common crus (data not shown). Thus, type O ears have dysmorphologies that are also seen in *Fgf10*- and *Fgfr2b*-null mutants (Pirvola et al., 2000; Pauley et al., 2003; Ohuchi et al., 2005) and are similar to those of *Fgf10* hypomorphs (X.W., T.J.W. and S.L.M., unpublished).

Fgf3 is expressed in tissues relevant for otic vesicle morphogenesis

To correlate *Fgf3* expression with major steps in early otic morphogenesis, we detected *Fgf3* transcripts by in situ hybridization of E8.5-10.5 embryos. Consistent with results described previously, at 3-4 somites *Fgf3* was expressed weakly in a dorsoventrally oriented stripe within the presumptive otic placode and strongly in the adjacent neurectoderm (data not shown) (but see McKay et al., 1996; Wright and Mansour, 2003). Ectodermal expression of *Fgf3* disappeared as the placode was induced and formed a cup (5-12 somites, data not shown), whereas neurectodermal expression remained strong throughout the otic cup stage and was restricted to r5-6 (Fig. 3A-D) (Mahmood et al., 1996; McKay et al., 1996; Wright and Mansour, 2003). As the cup closed to form the otic vesicle, hindbrain *Fgf3* became restricted to r6, expression was induced in an anteroventrolateral region of the vesicle and in delaminating neuroblasts of GVIII (Fig. 3E-H). EDS outgrowth was first evident morphologically at 27 somites, just as r6 expression of *Fgf3* diminished (Fig. 3I-L). At E10.5, *Fgf3* expression was maintained in anteroventrolateral otic cells from which both neuroblasts and sensory cells are derived (Fig. 3J,K) (Li et al., 1978; Carney and Silver, 1983). The neuroblasts of GVIII, however, no longer expressed *Fgf3*. Thus, *Fgf3* shows a dynamic pattern of expression in the hindbrain, GVIII and prospective sensory domains during the transition from the otic cup stage to the initiation of EDS outgrowth.

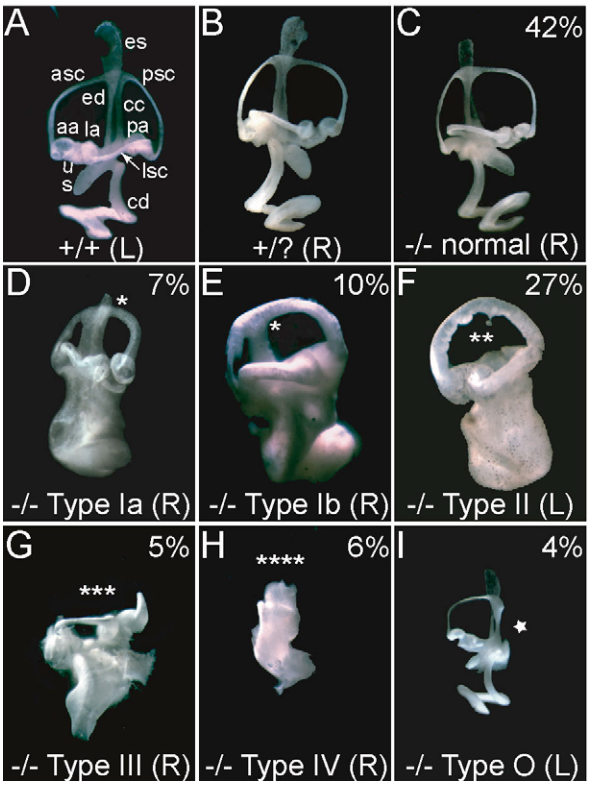

Fig. 2. The morphologies of *Fgf3* mutant inner ears fall into types of increasing severity. Lateral views of paint-filled inner ears from E15.5 control (**A**,**B**) and *Fgf3* mutant (**C-I**) mice. The percentage of each type among total mutants is indicated at the upper right. Asterisks and star (in I) indicate expected locations of missing structures. Ear side indicated by R (right) and L (left). Structures are labeled in the control left ear (A): aa, anterior ampulla; asc, anterior semicircular canal; cc, common crus; cd, cochlear duct; ed, endolymphatic duct; es, endolymphatic sac; la, lateral ampulla; lsc, lateral semicircular canal; pa, posterior ampulla; psc, posterior semicircular canal; s, saccule; u, utricle.

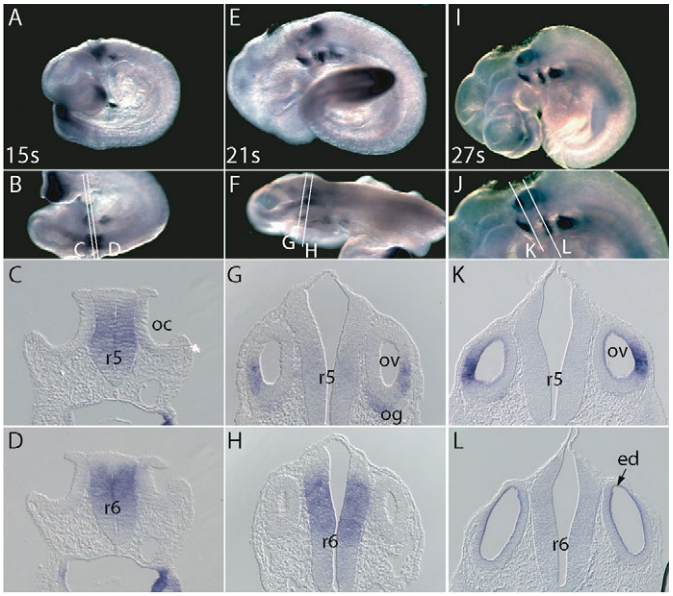

Fig. 3. *Fgf3* expression in tissues relevant for inner ear development. (**A-L**) Whole-mount mouse embryos probed with *Fgf3* and sectioned transversely. (A,E,I,J) Lateral views, somite numbers indicated at the lower left. (B,F) Dorsal views. Lines in B,F,J indicate the locations of sections C,D,G,H,K,L as labeled. r, hindbrain rhombomere; ov, otic vesicle; og, otic ganglion; ed, endolymphatic duct.

Dorsal otic gene expression is markedly affected in *Fgf3* mutants

The disruption of EDS development in the majority of abnormal *Fgf3* mutant ears suggested that molecular patterning of the dorsal otocyst could be perturbed. Thus, we analyzed expression of several dorsal otic markers at E9.5-10.5, the stage when otic vesicle morphogenesis is initiated by EDS outgrowth and when *Fgf3* expression is found in the hindbrain and initiates in the prosensory domain (Fig. 3). Again, both *Fgf3* mutant alleles were examined, but no allele-specific differences were apparent, so the results were combined (Fig. 4).

First, we analyzed genes whose mutant phenotypes included an EDS abnormality (*Gbx2* and *Dlx5*) (Depew et al., 1999; Lin et al., 2005) and/or were expressed in the developing EDS (*Wnt2b*). *Gbx2* expression, which marks a broad dorsomedial region of the vesicle, including the prospective EDS, as well as more anterior and posterior dorsal otic tissue, was generally not affected in E9.5 *Fgf3* mutants (Fig. 4A-B′). Only one such *Fgf3* mutant showed a slight reduction in the extent of the medial *Gbx2* domain (2/8 mutant ears, data not shown). The dorsomedial *Gbx2* expression domain persisted in E10.5 control inner ears (Fig. 4C,C′). By contrast, otic *Gbx2* expression was strongly affected by E10.5 in the *Fgf3* mutant otocysts, which were noticeably smaller than control otocysts (Fig. 4D,D′). In eight of 12 *Fgf3* mutant ears, no *Gbx2* staining was found in the otic epithelium (Fig. 4D,D′, right ear), and in the remaining four ears, weak staining was detected in the dorsomedial wall of the otocyst; however, the expression domain was severely reduced (Fig. 4D′, left ear). At E10.5, *Gbx2* was also expressed in the mid-hindbrain region (Lin et al., 2005). This *Gbx2* domain was not affected in any *Fgf3* mutant (Fig. 4C-D′). At E9.5, *Dlx5* was found in the dorsomedial otocyst of both controls and *Fgf3* mutants (Fig. 4E-F′). At E10.5, control otocysts showed initiation of EDS outgrowth and expression of *Dlx5* in the dorsal half of the otocyst (Fig. 4G,G′). However, in *Fgf3* mutants there was a slight reduction in the ventral boundary of the *Dlx5* domain, both medially and laterally, possibly owing to physical loss of the prospective EDS domain (n=6/6 ears; Fig. 4H,H′). *Wnt2b* was first detected in E10.5 control otocysts in a dorsomedial domain, marking the outgrowing EDS (Fig. 4I,I′). By contrast, *Wnt2b* was entirely absent from the dorsal otocyst in four of ten *Fgf3* mutant ears, and was severely reduced, showing only weak staining on the medial otocyst wall, in six of ten mutant ears, suggesting a failure of EDS specification (Fig. 4J,J′).

In addition, we studied *Hmx3* (*Nkx5.1*), a marker that broadly identifies the vestibular domain and is required redundantly with *Hmx2* (*Nkx5.2*) for vestibular development (Wang et al., 1998; Wang et al., 2001; Wang et al., 2004). *Hmx3* was expressed dorsolaterally in E10.5 control otocysts (Fig. 4K,K′), marking the prospective EDS and lateral canal plate regions. In *Fgf3* mutants, however, *Hmx3*

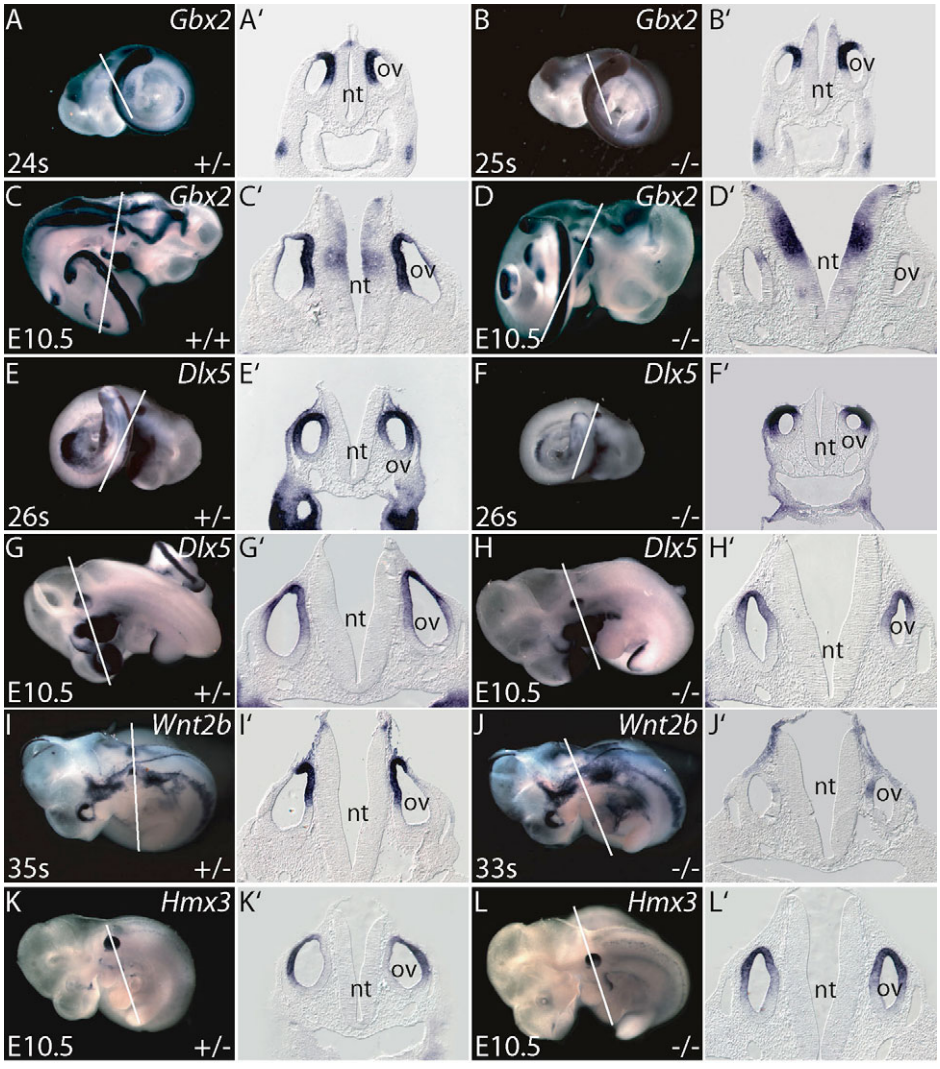

Fig. 4. Dorsal otic gene expression is markedly affected in *Fgf3* mutants after E9.5. Mouse embryos probed with *Gbx2* (**A-D**), *Dlx5* (**E-H**), *Wnt2b* (**I**,**J**) or *Hmx3* (**K**,**L**) were sectioned transversely (**A′-L′**) at the locations indicated by the white lines in A-L. Stage and genotype of each embryo are indicated at the lower left and right, respectively, of each whole-mount panel. ov, otic vesicle; nt, neural tube.

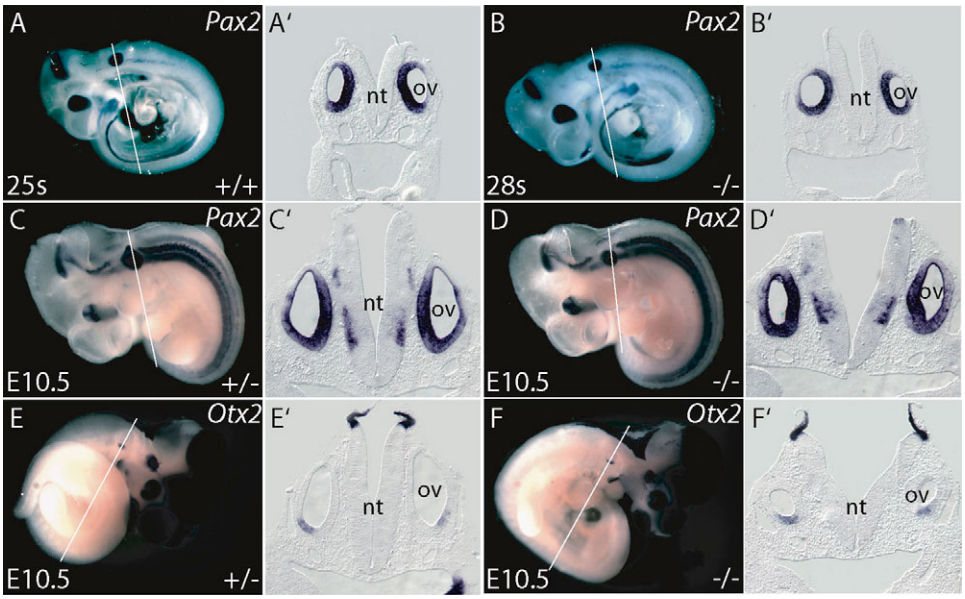

Fig. 5. Ventral otic markers are unaffected in *Fgf3* mutants. Whole-mount mouse embryos were probed with *Pax2* (**A**,**B**,**C**,**D**) or *Otx2* (**E**,**F**) and sectioned transversely (**A′-F′**) at the locations indicated by the white lines in A-F. Embryo stages and genotype abbreviations as for Fig. 4.

expression shifted medially (*n*=8/8 ears; Fig. 4L,L′). Finally, *Gata3*, which is expressed in both dorsolateral and ventromedial otocyst domains (Lawoko-Kerali et al., 2002; Lillevali et al., 2004) and is required for both dorsal and ventral otic development (Karis et al., 2001; Lillevali et al., 2006), was unaffected in E10 *Fgf3* mutants (data not shown), suggesting that its role in otic morphogenesis is independent of *Fgf3*.

Ventrally expressed otic genes important for cochlear development are not affected by loss of *Fgf3*

As the cochlear ducts in affected E15.5 *Fgf3* mutant inner ears were greatly enlarged and poorly coiled, we analyzed the expression patterns of ventral otic markers. *Pax2* marks the ventromedial region of the otocyst and is important for the development of the cochlear duct (Torres et al., 1996; Burton et al., 2004). *Pax2* expression was similar in control and *Fgf3* mutant embryos at E9.5 (Fig. 5A-B′) and E10.5 (Fig. 5C-D′). At E10.5, *Otx2* is normally expressed in a posterior ventrolateral patch (Morsli et al., 1998) (Fig. 5E,E′). In most *Fgf3* mutant ears, *Otx2* expression was unchanged (*n*=4/6 ears; Fig. 5F,F′). However, in one specimen, *Otx2* was reduced in one ear and absent in the other (data not shown). Finally, ventromedial *Gata3* expression was unaffected in *Fgf3* mutants (data not shown). Thus, it is likely that *Fgf3* mutant cochlear phenotypes are largely secondary to disturbances of dorsal patterning and morphogenesis.

Posterior sensory domain markers are downregulated in *Fgf3* mutants

Expression of *Fgf3* in the anteroventrolateral otocyst domain that gives rise to sensory cells and GVIII neuroblasts, together with the reduced size of GVIII in E11.5 $Fgf3^{neo}$ mutants, suggested roles for *Fgf3* in sensory organ and ganglion development (Mansour et al., 1993). Therefore, we assessed the expression of sensory markers, *Lfng* and *Bmp4*, and of a sensory and ganglion marker, *Fgf10*, in *Fgf3* mutant otocysts.

Lfng is normally expressed in the anteroventral otocyst – in the precursors of the cochlear, saccular and utricular sensory organs (Morsli et al., 1998). No significant differences in the distribution of *Lfng*-expressing cells were detected between control (Fig. 6A-A″) and mutant (Fig. 6B-B″) specimens at E10.5. *Bmp4* marks the presumptive cristae (Morsli et al., 1998). At E10.5, *Bmp4* expression was detected in two patches: one anterodorsolateral (Fig. 6C,C′) and the other posteroventral (Fig. 6C,C″). The anterior *Bmp4* patch contains precursors of the anterior and lateral cristae, whereas the posterior *Bmp4* domain (Fig. 6C, arrowhead) houses posterior crista precursors (Morsli et al., 1998). The anterior *Bmp4* domain was present in all E10.5 *Fgf3* mutant embryos (Fig. 6D,D′); however, there was a reduction in the extent of the staining and a ventral shift of that domain. The posterior *Bmp4* domain was not detected in four of six mutant inner ears (Fig. 6D,D″). Thus, loss of *Fgf3* can affect posterior crista development.

To assess GVIII development together with the prospective otic sensory domains, we examined *Fgf10* expression. At E9.5, *Fgf10* was expressed throughout both control and *Fgf3* mutant otocysts (data not shown). At E10.5, *Fgf10* was detected in the anterior pole of control vesicles, which includes the prospective sensory domain, and in delaminating neuroblasts of GVIII. *Fgf10* was also expressed in a second, smaller posterior patch, which gives rise to the posterior crista (Fig. 6E-E″) (Pauley et al., 2003). The posterior *Fgf10* domain appeared absent in eight of 12 *Fgf3* mutant ears (Fig. 6F, arrowhead), but examination of sections showed that it was shifted anteriorly and medially (Fig. 6F″). There was also a dorsomedial shift of the *Fgf10*-expressing anterior domain together with a corresponding positional shift of GVIII in six of 12 mutant ears (Fig. 6F′).

Fgf3 negatively regulates *Wnt3a* in r5-6

WNT signaling from the dorsal neural tube is required for dorsal otocyst patterning, with *Wnt1* and *Wnt3a* identified as the specific ligands (Riccomagno et al., 2005). We therefore examined *Wnt1* and *Wnt3a* expression in *Fgf3* mutants. As expected at E9.5, both *Wnt1* and *Wnt3a* expression marked the dorsal-most region of the developing neurectoderm in control embryos (Fig. 7A,A′,C,C′) (Parr et al., 1993). *Wnt1* expression was unchanged in all three *Fgf3* mutants examined (Fig. 7B,B′). Similarly, *Mafb* expression in r5-6 was unaffected in *Fgf3* mutants (data not shown). By contrast, all six *Fgf3* mutants examined showed a significant ventral expansion of *Wnt3a* expression in r5-6 (Fig. 7D,D″), but not in hindbrain regions anterior (Fig. 7D′) or posterior (Fig. 7D‴) to the otic vesicle. These results show that *Fgf3* negatively regulates *Wnt3a*, but not other genes required for otic development, in the dorsal hindbrain.

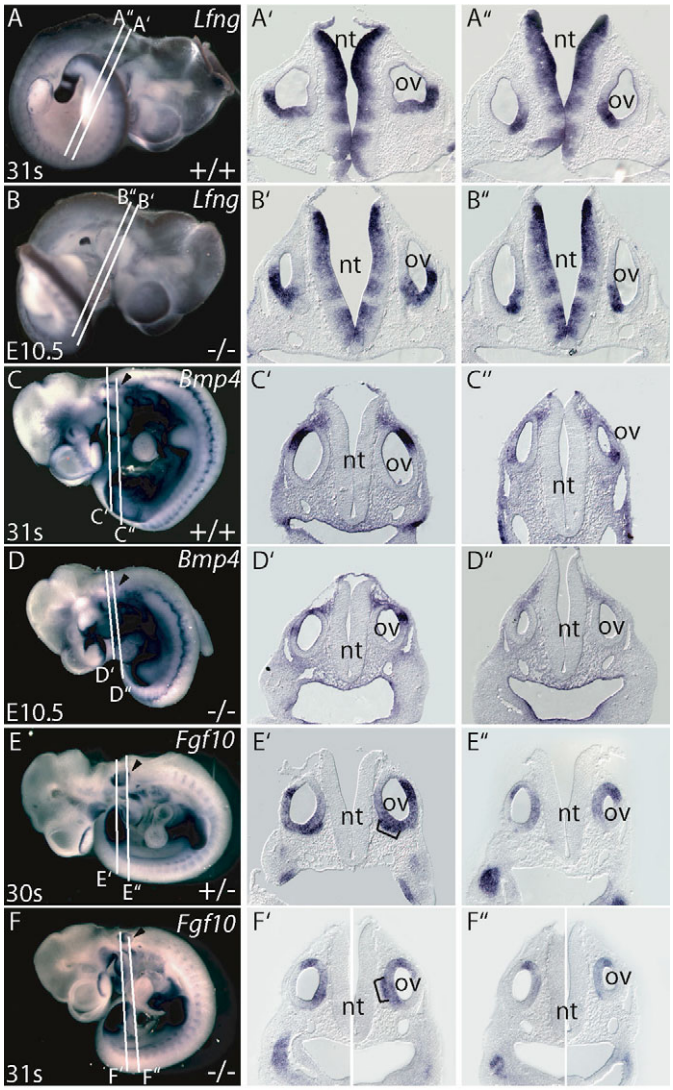

Fig. 6. Sensory and ganglion markers are affected in E10.5 *Fgf3* mutants. Whole-mount mouse embryos were probed with *Lfng* (**A**,**B**), *Bmp4* (**C**,**D**) and *Fgf10* (**E**,**F**) and sectioned transversely (**A′-F′**, anterior sections; **A″-F″**, posterior sections) at the locations indicated by the white lines in A-F. Arrowheads point to posterior expression domains of *Bmp4* (C,D) and *Fgf10* (E,F). Right and left ears in F′ and F″ are photographed separately owing to different sectioning angles. Brackets in E′ and F′ indicate the position of GVIII. Embryo stages and genotype abbreviations as for Fig. 4.

DISCUSSION

This study provides new morphologic data on aberrant inner ear morphogenesis in *Fgf3* mutants. These data, together with an analysis of changes in molecular patterning of *Fgf3* mutant otocysts and a comparison of similar studies of other mutants that affect inner ear morphogenesis, allow us to propose a placement for *Fgf3* in the genetic cascade leading to EDS formation and draw parallels with human inner ear dysmorphogenesis and deafness.

Fgf3 in inner ear morphogenesis

Although homozygotes for another *Fgf3*-null allele (*Fgf3*^{tm1Sng}, MGI:3027990) from which all coding sequences were removed, failed to show any inner ear abnormalities (Alvarez et al., 2003), we found that both *Fgf3* alleles examined here gave similar otic phenotypes. The phenotypic differences between our alleles and those of Alvarez and colleagues could arise either from differences in genetic background, or from the particular nature of the mutations, the contributions of which will require additional experiments.

We found that otic epithelia from two *Fgf3* mutant alleles exhibited a graded series of morphologies ranging from normal to complete loss of all vestibular structures. Common to all affected *Fgf3* mutant ears, except for those few members of the type O group, was hypoplasia or aplasia of the EDS, global swelling of the entire epithelium and poor cochlear coiling. Since the expression of ventral otocyst genes required for cochlear development was largely unperturbed, it is likely that the gross distortion of cochlear development was secondary to the effects on EDS and dorsal development. The association between abnormal EDS development and otic epithelial swelling is characteristic of both syndromic and non-syndromic human hearing loss (Wu et al., 2005) and is common to mouse mutations that disrupt the hindbrain signaling required for EDS induction (e.g. *Mafb*, *Hoxa1*, *Wnt1/Wnt3a* double mutants) (Pasqualetti et al., 2001; Riccomagno et al., 2005; Choo et al., 2006) or disrupt transcription factors that are expressed early in the dorsal otic vesicle and are required for EDS formation (e.g. *Gbx2*, *Hmx2*, *Hmx3*, *Dlx5*, *Dlx5/6*) (Wang et al., 2001; Merlo et al., 2002; Lin et al., 2005). Furthermore, mutations in *Foxi1*, which encodes an EDS-expressed transcription factor, or in its genetic target, *Slc26a4* (encoding the anion transporter, pendrin), cause abnormal EDS function, swelling of the entire epithelial space, loss of endocochlear potential and deafness (Everett et al., 2001; Hulander et al., 2003). Indeed, mutations in *SLC26A4* are a common cause of syndromic deafness (Pendred syndrome) and have also been found in non-syndromic deafness (DFNB4) (Morton and Nance, 2006). These patients show an enlarged vestibular aqueduct (the structure that houses the EDS) and may show the Mondini defect (dilatation and incomplete partitioning of the cochlear duct), similar to the *Fgf3* type Ia ears described here (Phelps et al., 1998; Fitoz et al., 2007). Thus, it appears that any disruption of EDS development, whether leading to EDS hypoplasia or aplasia, as when hindbrain-expressed or early otic-expressed genes are disrupted, or to overall dilatation of a labyrinth that retains an EDS, as in the case of later-acting EDS-expressed genes, can cause deafness. The EDS is thought to participate in regulation of endolymph homeostasis, which is crucial for hearing function in the mature ear, but the phenotypes exhibited by *Fgf3* and the other mutants with similar dysmorphologies suggest that EDS function might be required from the earliest stages of otic morphogenesis. It is interesting to speculate that Meniere's disease, an adult condition characterized by both auditory and vestibular symptoms and associated with enlarged endolymphatic spaces, could be caused either by mutations in EDS-expressed genes that function only after completion of morphogenesis, or by mutations in 'developmental' genes that, like *Fgf3*, have a wide spectrum of penetrance and expressivity.

EDS aplasia and general membranous swelling together with common crus aplasia was the most prevalent phenotypic complex (type II) observed in affected *Fgf3* mutant inner ears and has also been noted in some *Hoxb1*, *Mafb* and *Gbx2* mutants (Pasqualetti et al., 2001; Lin et al., 2005; Choo et al., 2006). Such a congenital phenotype has also been reported in patients (Manfre et al., 1997; Kim et al., 2004), but its cause is unknown. If EDS aplasia and consequent membranous swelling is explained by failure of FGF3-mediated signaling from the hindbrain to the dorsal otocyst, how might common crus aplasia arise? Since the common crus is formed

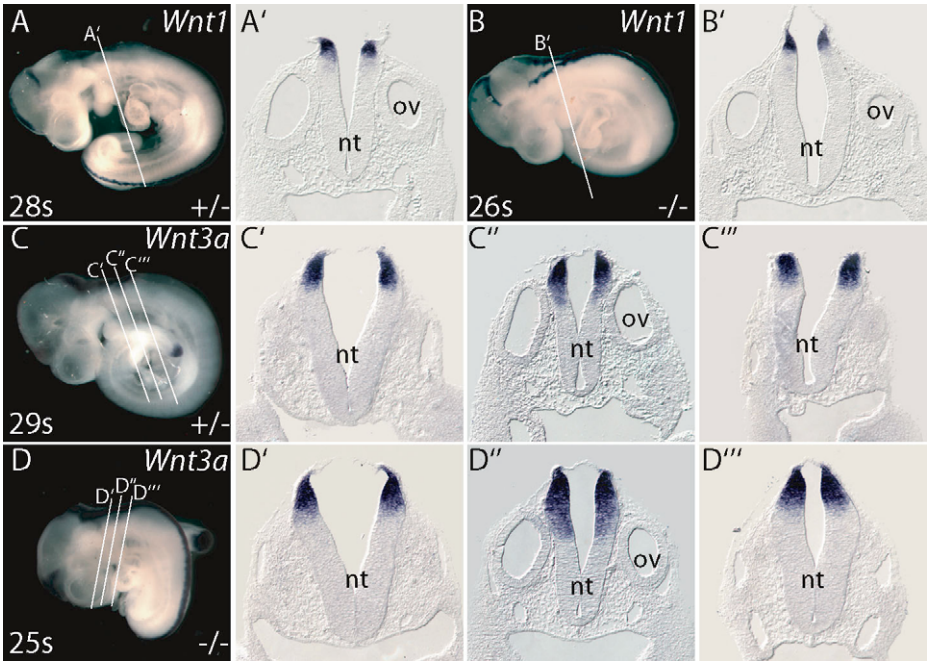

Fig. 7. Hindbrain expression of *Wnt3a*, but not *Wnt1*, expands ventrally in r5-6 of *Fgf3* mutants. Whole-mount mouse embryos were probed with *Wnt1* (**A**,**B**) or *Wnt3a* (**C**,**D**) and sectioned transversely (**A′**,**B′**, *Wnt1*; **C′**,**D′**, *Wnt3a* anterior; **C″**,**D″**, *Wnt3a* central; **C‴**,**D‴**, *Wnt3a* posterior) at the locations indicated by the labeled white lines in A-D. Embryo stages and genotype abbreviations as for Fig. 4.

when two distinct central regions of the vertical canal plate fuse and then resorb to form distinct anterior and posterior canals, one possibility is that *Fgf3*, expressed from the developing cristae, normally functions relatively directly to limit the fusion boundaries or the process of cellular resorption. Alternatively, it could be that the abnormal swelling of the epithelium consequent to failed or incomplete induction of the EDS is itself the cause of excessive cellular fusion and/or resorption in the vertical canal plate. Given the diversity of mutant genes that cause common crus aplasia, and the fact that most of these do not appear to be expressed in the otic epithelium, the latter possibility seems more likely. Conditional ablation of *Fgf3* in the otic epithelium versus hindbrain (work in progress) could help to address this issue.

FGF3 signaling maintains dorsal patterning of the otocyst

To understand the effects of the *Fgf3* mutations at the molecular level, we surveyed expression of regionally restricted otocyst genes in mutant embryos at a stage just prior to the first morphologic sign of aberrant vesicle development – namely, at EDS induction. Dorsally expressed genes were affected (absent or shifted), whereas ventrally expressed marker genes were not strongly affected, suggesting that *Fgf3* is a component of the dorsal determination pathway and EDS specification (Fig. 8). Just as the dysmorphologies of *Fgf3* mutant ears were similar to those of *Mafb*, *Hoxa1* and *Gbx2* mutants, so too were the trends for most of the molecular changes. Since *Mafb* and *Hoxa1* are required for *Fgf3* expression in the hindbrain (Carpenter et al., 1993; Frohman et al., 1993; McKay et al., 1996; Pasqualetti et al., 2001), and both *Mafb* and *Fgf3* are required for normal dorsal otic expression of *Gbx2* (Choo et al., 2006) (this study), this places *Fgf3* between *Mafb* and *Gbx2* in the EDS induction pathway. However, because *Gbx2* expression in *Fgf3* mutants was only strongly affected at E10.5, and not at E9.5, when *Gbx2* is affected in *Wnt1/Wnt3a* double mutants (which have no dorsal development at all) (Riccomagno et al., 2005), we suggest that WNTs provide the initiating signal for dorsal patterning of the otic vesicle, and that FGF3 directly or indirectly sustains or reinforces expression of dorsal otic genes. This might explain, at least in part, the reduced penetrance and severity of *Fgf3* otic morphologic and molecular phenotypes relative to those of *Gbx2*.

Expression of other dorsal otic genes downstream of *Gbx2* was also perturbed in *Fgf3* mutants. *Wnt2b*, the gene that most specifically marks the developing EDS, but the otic function of which is unknown, is absent from *Gbx2* mutant ears (Lin et al., 2005) and was strongly reduced or absent from *Fgf3* mutant ears, consistent with the EDS defects in both mutants. *Dlx5*, which normally marks the entire dorsal half of the otocyst and is required for both EDS and semicircular canal development (Merlo et al., 2002), was also affected in both mutants, but in slightly different ways. In *Gbx2* mutants, *Dlx5* is lost from the entire dorsomedial domain (Lin et al., 2005), whereas in *Fgf3* mutants, only the ventral-most region of both the dorsomedial and dorsolateral *Dlx5* domains were absent. This suggests that *Dlx5* might not be a direct target of FGF3 signaling, but is downstream of *Gbx2* and in this instance is revealing the loss of the dorsomedial EDS domain and the consequent dorsal shifts of its most ventromedial and ventrolateral domains. Finally, *Hmx3* is expressed in the dorsolateral otocyst and subsequently in the semicircular canals and is required for canal, but not for EDS, development (Wang et al., 2004). *Hmx3* expression is unchanged in *Gbx2* mutants (Lin et al., 2005) and slightly downregulated in *Wnt1/Wnt3a* double mutants (Riccomagno et al., 2005). By contrast, in *Fgf3* mutants there is a medial expansion of *Hmx3* expression, suggesting that *Fgf3* might normally function directly to restrict expansion of *Hmx3* into the medial otocyst or might function indirectly by restricting the *Wnt3a* domain dorsally.

Fgf3 does not have a unique role in ventral otic patterning

Despite abnormal cochlear development in *Fgf3* mutants, expression of *Pax2* and *Otx2*, ventral otic genes downstream of SHH signaling and necessary for cochlear development (Morsli et al., 1999; Riccomagno et al., 2002; Burton et al., 2004), were largely unaffected, except for one case of loss of *Otx2* expression. This was somewhat unexpected, given that both *Mafb* and *Gbx2* mutants show a medial expansion of otic *Otx2* expression (Lin et al., 2005; Choo

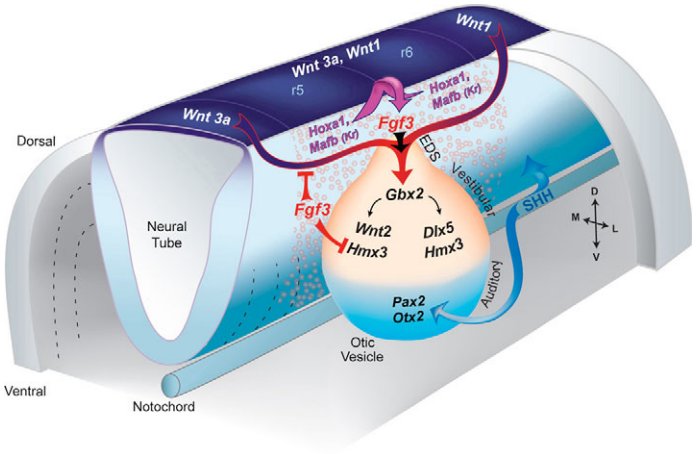

Fig. 8. Model for FGF3 function in otic morphogenesis initiation. Oblique view of the developing hindbrain and otic vesicle during initiation of otic morphogenesis. The model integrates present data with those published previously. Otic vesicle molecular patterning and morphogenesis are initiated by WNT signals provided redundantly by roofplate-expressed *Wnt3a* and *Wnt1* (dark blue). This signal induces otic *Gbx2*, which in turn induces *Wnt2* and *Dlx5* at a minimum, and is required for dorsal outgrowth of the EDS anlage. *Fgf3*, induced in r5-6 by *Hoxa1* and *Mafb* [*Mafb* (*Kr*)], serves to maintain otic *Gbx2* and its downstream genes, but has no direct effect on ventral otic genes (*Pax2* and *Otx2*). In addition, *Fgf3* prevents medial expansion of otic *Hmx3* and ventral expansion of hindbrain *Wnt3a*. The role of sonic hedgehog (SHH) in ventral otic patterning via induction of *Pax2* and *Otx2* is illustrated, but was not addressed here.

et al., 2006). However, since *Fgf3* appears to be required to maintain rather than to initiate *Gbx2* expression, it is possible that the early phase of *Gbx2* expression is sufficient to establish the *Otx2* domain and that FGF3, on its own, is not a major player in cochlear development. The possibility for redundant roles with *Fgf10*, such as occurs during otic induction, remains and will be tested using conditional mutants.

Fgf3 is required for posterior sensory domain and GVIII development

The *Bmp4* and *Fgf10* posterior expression domains marking the developing posterior cristae were absent or shifted dorsomedially, respectively, in *Fgf3* mutants. Although the vast majority of *Fgf3* mutant ears had a phenotype most consistent with a loss of FGF3 signaling resulting in a failure to properly induce the EDS, a small number of affected mutants apparently underwent normal EDS induction, but nevertheless developed with abnormal or absent posterior semicircular canals (type O). This phenotype is consistent with previous suggestions that FGF signals from the developing sensory patches induce non-sensory (canal) development (Chang et al., 2004) and further suggests that *Fgf3* might participate in posterior sensory domain specification. However, addressing this issue directly and assessing the relative contributions of *Fgf3* and *Fgf10* to posterior sensory and non-sensory development will require analysis of double conditional mutants in which the hindbrain requirement for *Fgf3* in EDS induction is bypassed.

As in the original study of $Fgf3^{neo}$ mutants, GVIII, as marked in this study by *Fgf10* expression, was notably smaller in affected mutant ears. We also consistently observed a dorsal shift of the ganglion in affected ears, as if either the neurogenic domain itself or the expression domain for an otocyst-derived attractant for delaminating GVIII neuroblasts had shifted. It is interesting that a similar dislocation of GVIII and the *Fgf3* expression domain was noted in studies of *Mafb* mutants (McKay et al., 1996).

Cross-talk between WNTs and FGFs in inner ear development

Our results show that *Fgf3* negatively regulates *Wnt3a* in the region of r5-6, preventing a ventral expansion of *Wnt3a* transcripts. This suggests an important role for *Fgf3* not only in reinforcing the inductive effect of WNT signals on the dorsal otocyst, but also in regulating localization of WNT signals to the dorsal-most region of the neural tube. Since WNT proteins are unlikely to diffuse over long distances, this localization may serve to limit the effects of WNTs to the dorsal otic vesicle.

FGF/WNT cross-talk is emerging as an important mechanism regulating various biological processes (Dailey et al., 2005), including brain, tooth and kidney development (Moon et al., 1997). In some cases, the parallel activation of FGF and WNT pathways causes developmental changes different from the individual effects of each factor, as exemplified by FGF/WNT interactions to specify neural and epidermal fate in the chick epiblast (Wilson et al., 2001). Evidence to support the role for FGFs in modulating WNT signaling comes from mouse genetic experiments showing that cross-regulation of FGF and WNT signaling is fundamental to normal skull development, when FGFs inhibit WNTs and subsequently osteoblast differentiation (Dailey et al., 2005). There are additional roles for cross-talk between the WNT and FGF pathways in otic development. During chick otic induction, mesodermal FGF19 induces neurectodermal expression of *Wnt8c* (Ladher et al., 2000). Both types of signals also participate in otic placode induction (Ladher et al., 2000; Wright and Mansour, 2003; Ladher et al., 2005), with WNT signals needed for stabilizing the otic placode cell state by enhancing and sensitizing the response of ectoderm to inductive FGF signaling (Ohyama et al., 2006). Given that WNT and FGF signaling pathway components continue to be expressed in the inner ear epithelia during the later stages of otic morphogenesis and sensory organ patterning, and that roles for each pathway are beginning to be defined (Pirvola et al., 2002; Pirvola et al., 2004; Wang et al., 2006; Hayashi et al., 2007), it will not be surprising if further intersections between these pathways are uncovered in the ear.

We thank Doris Wu for paint-fill instruction. cDNA clones newly obtained for this study were generously shared by Drs Eva Bober [*Hmx3* (*Nkx5.1*)], Doris Wu (*Lfng*), Andy McMahon (*Wnt1*), Jeffery Barrow (*Wnt3a*), Elisabeth Grove (*Wnt2b*), Mario Capecchi (*Bmp4*), Laure Bally-Cuif (*Otx2*) and Doug Engel (*Gata3*). Fred Grimmer provided helpful discussions of human inner ear dysmorphogenesis, Lisa Urness provided the *Fgf3*-hybridized embryos and Diana Lim created the model (Fig. 8). This manuscript was improved by suggestions from Lisa Urness and Gary Schoenwolf. This work was supported by grants from the NIDCD (R01DC05608 and R01DC04185) and by NIH Genetics Training Grant T32GM07464.

References

Alvarez, Y., Alonso, M. T., Vendrell, V., Zelarayan, L. C., Chamero, P., Theil, T., Bosl, M. R., Kato, S., Maconochie, M., Riethmacher, D. et al. (2003). Requirements for FGF3 and FGF10 during inner ear formation. *Development* **130**, 6329-6338.

Barald, K. F. and Kelley, M. W. (2004). From placode to polarization: new tunes in inner ear development. *Development* **131**, 4119-4130.

Bok, J., Bronner-Fraser, M. and Wu, D. K. (2005). Role of the hindbrain in dorsoventral but not anteroposterior axial specification of the inner ear. *Development* **132**, 2115-2124.

Burton, Q., Cole, L. K., Mulheisen, M., Chang, W. and Wu, D. K. (2004). The role of Pax2 in mouse inner ear development. *Dev. Biol.* **272**, 161-175.

Carney, P. R. and Silver, J. (1983). Studies on cell migration and axon guidance in the developing distal auditory system of the mouse. *J. Comp. Neurol.* **215**, 359-369.
Carpenter, E. M., Goddard, J. M., Chisaka, O., Manley, N. R. and Capecchi, M. R. (1993). Loss of Hox-A1 (Hox-1.6) function results in the reorganization of the murine hindbrain. *Development* **118**, 1063-1075.
Chang, W., Brigande, J. V., Fekete, D. M. and Wu, D. K. (2004). The development of semicircular canals in the inner ear: role of FGFs in sensory cristae. *Development* **131**, 4201-4211.
Choo, D., Ward, J., Reece, A., Dou, H., Lin, Z. and Greinwald, J. (2006). Molecular mechanisms underlying inner ear patterning defects in kreisler mutants. *Dev. Biol.* **289**, 308-317.
Cordes, S. P. and Barsh, G. S. (1994). The mouse segmentation gene kr encodes a novel basic domain-leucine zipper transcription factor. *Cell* **79**, 1025-1034.
Dailey, L., Ambrosetti, D., Mansukhani, A. and Basilico, C. (2005). Mechanisms underlying differential responses to FGF signaling. *Cytokine Growth Factor Rev.* **16**, 233-247.
Depew, M. J., Liu, J. K., Long, J. E., Presley, R., Meneses, J. J., Pedersen, R. A. and Rubenstein, J. L. (1999). Dlx5 regulates regional development of the branchial arches and sensory capsules. *Development* **126**, 3831-3846.
Dressler, G. R., Deutsch, U., Chowdhury, K., Nornes, H. O. and Gruss, P. (1990). Pax2, a new murine paired-box-containing gene and its expression in the developing excretory system. *Development* **109**, 787-795.
Everett, L. A., Belyantseva, I. A., Noben-Trauth, K., Cantos, R., Chen, A., Thakkar, S. I., Hoogstraten-Miller, S. L., Kachar, B., Wu, D. K. and Green, E. D. (2001). Targeted disruption of mouse Pds provides insight about the inner-ear defects encountered in Pendred syndrome. *Hum. Mol. Genet.* **10**, 153-161.
Fekete, D. M. and Wu, D. K. (2002). Revisiting cell fate specification in the inner ear. *Curr. Opin. Neurobiol.* **12**, 35-42.
Fitoz, S., Sennaroglu, L., Incesulu, A., Cengiz, F. B., Koc, Y. and Tekin, M. (2007). SLC26A4 mutations are associated with a specific inner ear malformation. *Int. J. Pediatr. Otorhinolaryngol.* **71**, 479-486.
Fritzsch, B., Pauley, S. and Beisel, K. W. (2006). Cells, molecules and morphogenesis: the making of the vertebrate ear. *Brain Res.* **1091**, 151-171.
Frohman, M. A., Martin, G. R., Cordes, S. P., Halamek, L. P. and Barsh, G. S. (1993). Altered rhombomere-specific gene expression and hyoid bone differentiation in the mouse segmentation mutant, kreisler (kr). *Development* **117**, 925-936.
George, K. M., Leonard, M. W., Roth, M. E., Lieuw, K. H., Kioussis, D., Grosveld, F. and Engel, J. D. (1994). Embryonic expression and cloning of the murine GATA-3 gene. *Development* **120**, 2673-2686.
Grove, E. A., Tole, S., Limon, J., Yip, L. and Ragsdale, C. W. (1998). The hem of the embryonic cerebral cortex is defined by the expression of multiple Wnt genes and is compromised in Gli3-deficient mice. *Development* **125**, 2315-2325.
Hayashi, T., Cunningham, D. and Bermingham-McDonogh, O. (2007). Loss of Fgfr3 leads to excess hair cell development in the mouse organ of Corti. *Dev. Dyn.* **236**, 525-533.
Henrique, D., Adam, J., Myat, A., Chitnis, A., Lewis, J. and Ish-Horowicz, D. (1995). Expression of a Delta homologue in prospective neurons in the chick. *Nature* **375**, 787-790.
Hulander, M., Kiernan, A. E., Blomqvist, S. R., Carlsson, P., Samuelsson, E. J., Johansson, B. R., Steel, K. P. and Enerback, S. (2003). Lack of pendrin expression leads to deafness and expansion of the endolymphatic compartment in inner ears of Foxi1 null mutant mice. *Development* **130**, 2013-2025.
Hutson, M. R., Lewis, J. E., Nguyen-Luu, D., Lindberg, K. H. and Barald, K. F. (1999). Expression of Pax2 and patterning of the chick inner ear. *J. Neurocytol.* **28**, 795-807.
Jones, C. M., Lyons, K. M. and Hogan, B. L. (1991). Involvement of Bone Morphogenetic Protein-4 (BMP-4) and Vgr-1 in morphogenesis and neurogenesis in the mouse. *Development* **111**, 531-542.
Karis, A., Pata, I., van Doorninck, J. H., Grosveld, F., de Zeeuw, C. I., de Caprona, D. and Fritzsch, B. (2001). Transcription factor GATA-3 alters pathway selection of olivocochlear neurons and affects morphogenesis of the ear. *J. Comp. Neurol.* **429**, 615-630.
Kiernan, A. E., Steel, K. P. and Fekete, D. M. (2002). Development of the mouse inner ear. In *Mouse Development: Patterning, Morphogenesis, and Organogenesis* (ed. J. Rossant and P. P. L. Tam), pp. 539-566. San Diego: Academic Press.
Kim, H. J., Song, J. W., Chon, K. M. and Goh, E. K. (2004). Common crus aplasia: diagnosis by 3D volume rendering imaging using 3DFT-CISS sequence. *Clin. Radiol.* **59**, 830-834.
Ladher, R. K., Anakwe, K. U., Gurney, A. L., Schoenwolf, G. C. and Francis-West, P. H. (2000). Identification of synergistic signals initiating inner ear development. *Science* **290**, 1965-1967.
Ladher, R. K., Wright, T. J., Moon, A. M., Mansour, S. L. and Schoenwolf, G. C. (2005). FGF8 initiates inner ear induction in chick and mouse. *Genes Dev.* **19**, 603-613.
Lawoko-Kerali, G., Rivolta, M. N. and Holley, M. (2002). Expression of the transcription factors GATA3 and Pax2 during development of the mammalian inner ear. *J. Comp. Neurol.* **442**, 378-391.
Li, C. W., Van De Water, T. R. and Ruben, R. J. (1978). The fate mapping of the eleventh and twelfth day mouse otocyst: an in vitro study of the sites of origin of the embryonic inner ear sensory structures. *J. Morphol.* **157**, 249-267.
Lillevali, K., Matilainen, T., Karis, A. and Salminen, M. (2004). Partially overlapping expression of Gata2 and Gata3 during inner ear development. *Dev. Dyn.* **231**, 775-781.
Lillevali, K., Haugas, M., Matilainen, T., Pussinen, C., Karis, A. and Salminen, M. (2006). Gata3 is required for early morphogenesis and Fgf10 expression during otic development. *Mech. Dev.* **123**, 415-429.
Lin, Z., Cantos, R., Patente, M. and Wu, D. (2005). *Gbx2* is required for the morphogenesis of the mouse inner ear: a downstream target of hindbrain signaling. *Development* **132**, 2309-2318.
Mafong, D. D., Shin, E. J. and Lalwani, A. K. (2002). Use of laboratory evaluation and radiologic imaging in the diagnostic evaluation of children with sensorineural hearing loss. *Laryngoscope* **112**, 1-7.
Mahmood, R., Mason, I. J. and Morriss-Kay, G. M. (1996). Expression of Fgf-3 in relation to hindbrain segmentation, otic pit position and pharyngeal arch morphology in normal and retinoic acid-exposed mouse embryos. *Anat. Embryol.* **194**, 13-22.
Manfre, L., Genuardi, P., Tortorici, M. and Lagalla, R. (1997). Absence of the common crus in Goldenhar syndrome. *AJNR Am. J. Neuroradiol.* **18**, 773-775.
Mansour, S. L. and Schoenwolf, G. C. (2005). Morphogenesis of the inner ear. In *Development of the Inner Ear* (ed. M. W. Kelley, D. K. Wu, A. N. Popper and R. R. Fay), pp. 43-84. New York: Springer-Verlag.
Mansour, S. L., Goddard, J. M. and Capecchi, M. R. (1993). Mice homozygous for a targeted disruption of the proto-oncogene int-2 have developmental defects in the tail and inner ear. *Development* **117**, 13-28.
McKay, I. J., Lewis, J. and Lumsden, A. (1996). The role of FGF-3 in early inner ear development: an analysis in normal and kreisler mutant mice. *Dev. Biol.* **174**, 370-378.
Merlo, G. R., Paleari, L., Mantero, S., Zerega, B., Adamska, M., Rinkwitz, S., Bober, E. and Levi, G. (2002). The Dlx5 homeobox gene is essential for vestibular morphogenesis in the mouse embryo through a BMP4-mediated pathway. *Dev. Biol.* **248**, 157-169.
Moon, R. T., Brown, J. D. and Torres, M. (1997). WNTs modulate cell fate and behavior during vertebrate development. *Trends Genet.* **13**, 157-162.
Morsli, H., Choo, D., Ryan, A., Johnson, R. and Wu, D. K. (1998). Development of the mouse inner ear and origin of its sensory organs. *J. Neurosci.* **18**, 3327-3335.
Morsli, H., Tuorto, F., Choo, D., Postiglione, M. P., Simeone, A. and Wu, D. K. (1999). Otx1 and Otx2 activities are required for the normal development of the mouse inner ear. *Development* **126**, 2335-2343.
Morton, C. C. and Nance, W. E. (2006). Newborn hearing screening – a silent revolution. *N. Engl. J. Med.* **354**, 2151-2164.
Ohuchi, H., Yasue, A., Ono, K., Sasaoka, S., Tomonari, S., Takagi, A., Itakura, M., Moriyama, K., Noji, S. and Nohno, T. (2005). Identification of cis-element regulating expression of the mouse Fgf10 gene during inner ear development. *Dev. Dyn.* **233**, 177-187.
Ohyama, T., Mohamed, O. A., Taketo, M. M., Dufort, D. and Groves, A. K. (2006). Wnt signals mediate a fate decision between otic placode and epidermis. *Development* **133**, 865-875.
Parr, B. A., Shea, M. J., Vassileva, G. and McMahon, A. P. (1993). Mouse Wnt genes exhibit discrete domains of expression in the early embryonic CNS and limb buds. *Development* **119**, 247-261.
Pasqualetti, M., Neun, R., Davenne, M. and Rijli, F. M. (2001). Retinoic acid rescues inner ear defects in Hoxa1 deficient mice. *Nat. Genet.* **29**, 34-39.
Pauley, S., Wright, T. J., Pirvola, U., Ornitz, D., Beisel, K. and Fritzsch, B. (2003). Expression and function of FGF10 in mammalian inner ear development. *Dev. Dyn.* **227**, 203-215.
Phelps, P. D., Coffey, R. A., Trembath, R. C., Luxon, L. M., Grossman, A. B., Britton, K. E., Kendall-Taylor, P., Graham, J. M., Cadge, B. C., Stephens, S. G. et al. (1998). Radiological malformations of the ear in Pendred syndrome. *Clin. Radiol.* **53**, 268-273.
Pirvola, U., Spencer-Dene, B., Xing-Qun, L., Kettunen, P., Thesleff, I., Fritzsch, B., Dickson, C. and Ylikoski, J. (2000). FGF/FGFR-2(IIIb) signaling is essential for inner ear morphogenesis. *J. Neurosci.* **20**, 6125-6134.
Pirvola, U., Ylikoski, J., Trokovic, R., Hebert, J. M., McConnell, S. K. and Partanen, J. (2002). FGFR1 is required for the development of the auditory sensory epithelium. *Neuron* **35**, 671-680.
Pirvola, U., Zhang, X., Mantela, J., Ornitz, D. M. and Ylikoski, J. (2004). Fgf9 signaling regulates inner ear morphogenesis through epithelial-mesenchymal interactions. *Dev. Biol.* **273**, 350-360.
Riccomagno, M. M., Martinu, L., Mulheisen, M., Wu, D. K. and Epstein, D. J. (2002). Specification of the mammalian cochlea is dependent on Sonic hedgehog. *Genes Dev.* **16**, 2365-2378.
Riccomagno, M. M., Takada, S. and Epstein, D. J. (2005). Wnt-dependent regulation of inner ear morphogenesis is balanced by the opposing and supporting roles of Shh. *Genes Dev.* **19**, 1612-1623.
Simeone, A., Acampora, D., Mallamaci, A., Stornaiuolo, A., D'Apice, M. R., Nigro, V. and Boncinelli, E. (1993). A vertebrate gene related to

orthodenticle contains a homeodomain of the bicoid class and demarcates anterior neuroectoderm in the gastrulating mouse embryo. *EMBO J.* **12**, 2735-2747.

Smith, R. J., Bale, J. F., Jr and White, K. R. (2005). Sensorineural hearing loss in children. *Lancet* **365**, 879-890.

Stark, M. R., Biggs, J. J., Schoenwolf, G. C. and Rao, M. S. (2000). Characterization of avian frizzled genes in cranial placode development. *Mech. Dev.* **93**, 195-200.

Torres, M., Gomez-Pardo, E. and Gruss, P. (1996). Pax2 contributes to inner ear patterning and optic nerve trajectory. *Development* **122**, 3381-3391.

Wang, W., Van De Water, T. and Lufkin, T. (1998). Inner ear and maternal reproductive defects in mice lacking the Hmx3 homeobox gene. *Development* **125**, 621-634.

Wang, W., Chan, E. K., Baron, S., Van de Water, T. and Lufkin, T. (2001). Hmx2 homeobox gene control of murine vestibular morphogenesis. *Development* **128**, 5017-5029.

Wang, W., Grimmer, J. F., Van De Water, T. R. and Lufkin, T. (2004). Hmx2 and Hmx3 homeobox genes direct development of the murine inner ear and hypothalamus and can be functionally replaced by Drosophila Hmx. *Dev. Cell* **7**, 439-453.

Wang, Y., Guo, N. and Nathans, J. (2006). The role of Frizzled3 and Frizzled6 in neural tube closure and in the planar polarity of inner-ear sensory hair cells. *J. Neurosci.* **26**, 2147-2156.

Wassarman, K. M., Lewandoski, M., Campbell, K., Joyner, A. L., Rubenstein, J. L., Martinez, S. and Martin, G. R. (1997). Specification of the anterior hindbrain and establishment of a normal mid/hindbrain organizer is dependent on Gbx2 gene function. *Development* **124**, 2923-2934.

Wilkinson, D. G., Peters, G., Dickson, C. and McMahon, A. P. (1988). Expression of the FGF-related proto-oncogene int-2 during gastrulation and neurulation in the mouse. *EMBO J.* **7**, 691-695.

Wilson, S. I., Rydstrom, A., Trimborn, T., Willert, K., Nusse, R., Jessell, T. M. and Edlund, T. (2001). The status of Wnt signalling regulates neural and epidermal fates in the chick embryo. *Nature* **411**, 325-330.

Wright, T. J. and Mansour, S. L. (2003). Fgf3 and Fgf10 are required for mouse otic placode induction. *Development* **130**, 3379-3390.

Wu, C. C., Chen, Y. S., Chen, P. J. and Hsu, C. J. (2005). Common clinical features of children with enlarged vestibular aqueduct and Mondini dysplasia. *Laryngoscope* **115**, 132-137.

Xu, X., Weinstein, M., Li, C., Naski, M., Cohen, R. I., Ornitz, D. M., Leder, P. and Deng, C. (1998). Fibroblast growth factor receptor 2 (FGFR2)-mediated reciprocal regulation loop between FGF8 and FGF10 is essential for limb induction. *Development* **125**, 753-765.

Zelarayan, L. C., Vendrell, V., Alvarez, Y., Dominguez-Frutos, E., Theil, T., Alonso, M. T., Maconochie, M. and Schimmang, T. (2007). Differential requirements for FGF3, FGF8 and FGF10 during inner ear development. *Dev. Biol*. **130**, 6329-6338.

Zheng, Q. Y., Johnson, K. R. and Erway, L. C. (1999). Assessment of hearing in 80 inbred strains of mice by ABR threshold analyses. *Hear. Res.* **130**, 94-107.